

The Latitudinal Variation in the Wind-Speed Parameterization of Oceanic Whitecap Coverage; Implications for Global Modelling of Air-Sea Gas Flux and Sea Surface Aerosol Generation

By

Edward C. Monahan<sup>1</sup>, Giles Hooker<sup>2</sup> and Christopher J. Zappa<sup>3</sup>

- 1) Department of Marine Sciences, University of Connecticut at Avery Point
- 2) Department of Statistical Science, Cornell University, Ithaca, NY
- 3) Lamont-Doherty Earth Observatory, Columbia University, Palisades, NY

In a recent publication Salisbury et al (2014) compared their estimates of oceanic whitecap coverage, derived from microwave measurements taken by satellite-borne radiometers, with whitecap coverage deduced from the application of one of the wind speed power-law parameterizations found in Monahan and O'Muircheartaigh (1980). Specifically, they compare their global maps of whitecap coverage with those determined using for  $n$ , the power-law exponent in Eq. 1, the value of 3.41, as obtained by Monahan and

$$W_B = C U^n, \text{ where } U \text{ is the 10-meter elevation wind speed. Eq.1}$$

O'Muircheartaigh via the application of the technique of robust biweight fitting to the whitecap data found in Monahan (1971) and Toba and Chaen (1973). A comparison between the whitecap coverage as deduced at a microwave frequency of 37GHz and that deduced using Eq.1 above is found in Fig. 3b of Salisbury et al (2014). We focus on this comparison as the microwave measurements at this frequency detect whitecap foam as thin as 1 mm, and thus should correspond roughly to the Stage B whitecaps (decaying foam patches) analyzed by Monahan and O'Muircheartaigh (1980). It is apparent from this figure of Salisbury et al that MM80 (their notation) overestimates whitecap coverage at both the high northern and high southern latitudes. Those authors conclude that Eq.1 incorporates too high a wind speed dependence of whitecap coverage at such high latitudes. This conclusion is consistent with the discussion found in Monahan and O'Muircheartaigh (1986) where, looking at the  $n$ 's associated with 5 data sets, they detected a diminution in  $n$  with decreasing surface sea water temperature (SST), and concluded that this was a reflection of the general decrease in SST with increase in latitude. (MM86 attributed this latitude dependence of  $n$  primarily on the latitudinal variation of the characteristic duration of high wind speed events.)

The current authors have, in the work presented here, made use of 14 Stage B whitecap data sets (each resulting from the manual analysis of photographs), and 1 data set recently collected in the Southern Ocean involving high resolution digital images (and the use of an automatic analysis protocol). A simplified listing of the relevant Southern Ocean whitecap data can be found in Appendix A of this paper.

The initial test involved using all of the non-null  $W_B, U$  data points from these 15 data sets, having first sorted them into two categories by temperature, i.e.  $SST > 15^{\circ}C$  and  $SST < 15^{\circ}C$ . The result is illustrated in Fig. 1, where the  $n(SST > 15^{\circ}) = 3.53$ , and the  $n(SST < 15^{\circ}) = 2.89$ . It is noted that Monahan and O’Muircheartaigh(1980), analyzing only two  $W_b$  data sets, for both of which  $SST > 15^{\circ}C$ , by ordinary least squares fitting, had arrived at an n-value of 3.52. It should also be noted that these n-values are all greater than the n-values obtained by Salisbury et al (2014) for their  $W_{37}$ (and  $W_{10}$ ) power-laws.

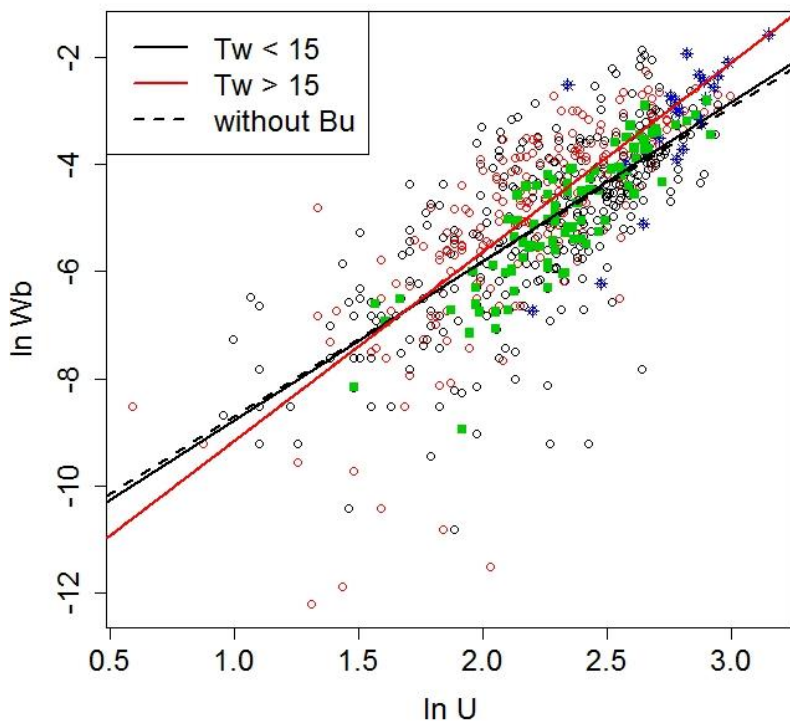


Figure 1.  $\ln W_B$  vs  $\ln U$ , for  $SST > 15^{\circ}C$  and  $SST < 15^{\circ}C$ . Green dots: from high resolution digital imagery taken in the Southern Ocean.

The slopes of these two lines on this log-log plot, i.e. the two n’s, are significantly different ( $P = 0.01625$ ).

A further analysis was conducted using that subset of 8  $W_B$ -data sets for which the current authors had information on the mean latitude of the observations. A three-dimensional graphical summary of these results is shown in Fig. 2. Note here that results from both hemispheres are plotted along the same branch of the x axis, i.e. what is plotted here is the absolute value of latitude. When one looks at the intersection of the gray "data surface" in this figure with the left-hand (high (absolute) Lat.) wall of this "data cube" one sees

that the slope of this intersection, i.e. the high Lat.  $n$ , is much less than the slope of the intersection of this "data surface" with the right-hand (low (absolute) Lat.) wall of this "data cube", i.e. the low Lat.  $n$ . Thus we see that  $n$  does decrease with increasing (absolute) latitude. It should be acknowledged that the "twist" with latitude of this "data surface" is only marginally significant, but it is consistent with the findings illustrated in Fig. 1, where the difference between the "cold water" and "warm water"  $n$ 's is significantly different.

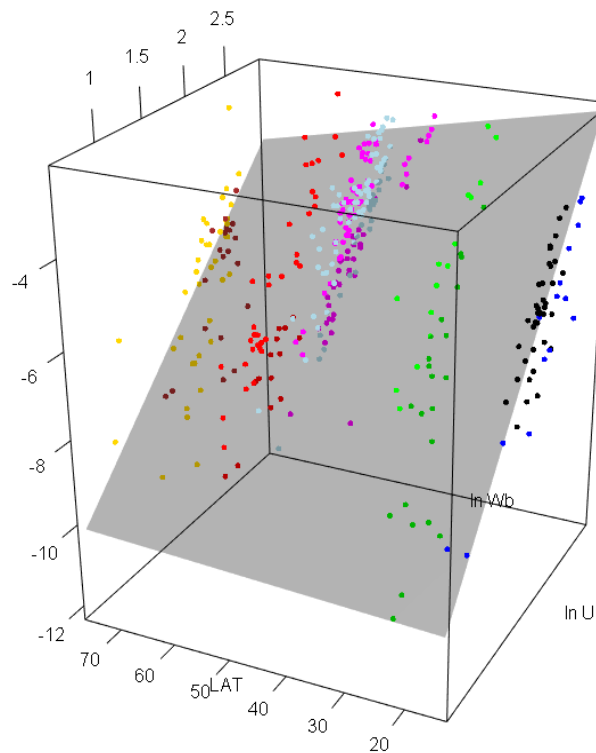


Figure 2. 3-D plot of absolute latitude (x-axis);  $\ln U$ , where  $U$  is the 10 m-elevation wind speed (y-axis); and  $\ln W_B$ , where  $W_B$  is the simple fraction of the sea surface covered by decaying foam patches (z-axis). Key: BOMEX+ = black, BOMEX(Flip) = blue, S. China Sea (Toba & Chaen) = green, JASIN = red, MIZEX83 = brown, MIZEX84 = gold, STREX (Doyle) = light blue, and Southern Ocean (Zappa) = magenta.

A series of air-sea gas transfer models, beginning with Monahan and Spillane (1984), have parameterized the gas transfer coefficient, or "friction velocity", explicitly in terms of the fraction of the sea surface covered by Stage B (current usage) whitecaps. If such a model is to be evaluated where, of necessity, wind

speed is being used as a surrogate for  $W_B$ , then it is critical that the latitude-appropriate exponent,  $n$ , be used in assessing  $W_B$  from Eq. 1. Most of the early studies of  $k$ (trans. coeff.) as a function of  $W_B$  used photographs, or digital systems working in the visible portion of the E-M spectrum, to estimate  $W_B$ . If  $W_{37}$ , or some other microwave frequency measurement of whitecapping, is to be substituted in such parameterizations for  $k$ , a robust relationship, i.e. an inter-calibration, between  $W_B$  and  $W_{\mu\text{wave}}$  need be established.

Grythe et al (2014) and others have recently concluded that the Monahan et al (1986) sea surface aerosol source function is still "the most widely used source function", and one of the terms in this function is  $W_B$ . While clearly the substitution in this function, or in modifications of it, of a climatologically derived  $W_B$ -expression, or  $W_B$ -values from satellite-derived synoptic maps, is to be encouraged, but again a clearer understanding of the  $W_B, W_{\mu\text{wave}}$  relationship is needed.

### Acknowledgments

E.C.M.'s research on whitecaps, sea spray, and gas exchange is currently supported via NSF Grant AGS-1356541. C.J.Z.'s participation in the Southern Ocean Gas Exchange Experiment was supported via NSF Grant OCE-0647667 and NOAA award NA07OAR4310094.

### References

Grythe, H., J. Ström, R. Krejci, P. Quinn, and A. Stohl (2014), A review of sea-spray aerosol source functions using a large global set of sea salt aerosol concentration measurements, *Atmos. Chem. Phys.*, **14**, 1277-1297, doi:10.5194/acp-14-1277-2014.

Monahan, E.C. (1971), Oceanic whitecaps, *J. Phys. Oceanogr.*, **1**, 139-144.

Monahan, E.C. and I.G. O'Muircheartaigh (1980), Optimal power-law description of oceanic whitecap coverage dependence on wind speed, *J. Phys. Oceanogr.*, **10**, 2094-2099.

Monahan, E.C. and I.G. O'Muircheartaigh (1986), Whitecaps and the passive remote sensing of the ocean surface, *Internat. J. Rem. Sens.*, **7**, 627-642.

Monahan, E.C., D.E. Spiel, and K.L. Davidson (1986), A model of marine aerosol generation via whitecaps and wave disruption, Oceanic Whitecaps and Their Role in Air-Sea Exchange Processes, E.C. Monahan and G. MacNiocaill, eds., Springer, 167-174.

Monahan, E.C., and M.C. Spillane (1984), The role of oceanic whitecaps in air-sea gas exchange, Gas Transfer at Water Surfaces, W. Brutsaert and G.J. Jirka, eds., Springer, 495-503.

Salisbury, D.J., M.D. Anguelova, and I.M. Brooks (2014), Global distribution and seasonal dependence of satellite-based whitecap fraction, *Geophys. Res. Lett.*, **41**, 1616-1623, doi:10.1002/2014GL059246.

Toba, Y. and M. Chaen (1973), Quantitative expression of the breaking of wind waves on the sea surface, *Rec. of Oceanogr. Works Japan*, **12**, 1-11.

Appendix A: Table of Southern Ocean GasEx Whitecap Data

Obs. No.	U(m/sec)	T <sub>A</sub> (°C)	T <sub>w</sub> (°C)	W <sub>B</sub> <sup>1</sup>
1	7.2	5.27	6.33	0.00134
2	10.7	5.01	5.31	0.00456
3	8.2	3.89	3.36	0.00121
6 <sup>2</sup>	11.8	8.02	6.20	0.00637
7	9.9	7.50	6.50	0.00368
8	11.2	6.02	5.21	0.00410
9	11.0	6.03	5.91	0.00453
10	10.2	8.89	5.82	0.00237
11	10.3	7.71	5.65	0.00244
12	9.3	6.38	5.69	0.00397
13	11.8	6.60	5.43	0.00522
14	10.3	6.41	5.41	0.00510
15	10.4	6.51	5.74	0.00571
16	9.6	6.60	5.69	0.01051
17	9.6	7.09	5.61	0.00290
19	8.5	6.81	5.58	0.01029
20	5.0	7.72	5.73	0.00097
21	7.2	8.38	5.99	0.00184
22	9.6	5.24	5.72	0.00264
23	8.3	5.40	5.62	0.00250
24	8.4	3.27	2.65	0.00172
25	14.2	3.05	2.91	0.02752
26	14.6	3.04	2.98	0.03284
27	14.4	2.81	3.14	0.02463
28	13.9	2.68	3.19	0.03156
29	12.4	2.09	3.29	0.01674
30	9.6	2.97	3.22	0.00182
31	12.1	4.09	3.20	0.00642
33	11.0	3.15	3.26	0.01107

34	12.9	6.72	5.76	0.01493
35	13.6	6.59	5.86	0.01056
36	8.4	6.15	5.17	0.00470
37	11.4	4.99	4.99	0.01135
38	9.1	5.83	4.96	0.00591
39	9.9	5.70	4.95	0.00707
40	7.8	5.35	5.01	0.00117
43	13.2	2.49	4.84	0.03038
45	12.6	3.15	5.03	0.02785
46	14.8	6.47	4.79	0.03566
47	14.9	6.67	4.79	0.03307
48	13.6	7.02	4.81	0.02481
49	13.2	6.71	4.79	0.01609
50	13.3	6.86	4.77	0.01218
51	7.8	4.09	4.60	0.00085
53	7.0	2.55	4.97	0.00079
55	8.7	4.09	4.90	0.00427
56	9.2	3.77	4.83	0.01232
57	9.9	3.95	4.01	0.00852
59	9.0	5.08	4.88	0.00400
60	8.3	5.22	4.90	0.00258
61	9.6	5.22	4.90	0.00654
62	10.6	4.69	4.87	0.00565
63	9.8	4.93	4.92	0.00437
64	11.8	3.43	5.22	0.01127
65	11.6	3.37	4.88	0.01623
66	10.4	3.17	4.90	0.01289
67	13.4	3.37	4.84	0.03775
68	14.2	3.18	4.76	0.05481
69	10.5	1.96	4.86	0.01680
70	9.6	1.82	4.75	0.01503
71	9.8	1.84	4.78	0.01378
72	8.8	1.91	4.77	0.01214
73	8.2	1.99	4.77	0.00660
74	8.5	2.25	4.76	0.00647
75	10.8	6.19	4.89	0.00894
76	9.9	5.39	4.77	0.00627
77	9.9	3.17	4.53	0.00741
82	7.7	2.18	4.85	0.00277
83	10.6	2.21	4.77	0.01684
84	10.4	2.63	4.82	0.01085
85	11.4	3.20	5.00	0.01406
86	7.1	4.45	4.91	0.00247
87	4.4	5.20	5.09	0.00029

88	4.8	5.29	5.19	0.00136
89	5.3	5.03	5.33	0.00150
91	6.5	5.57	4.77	0.00121
92	8.9	5.63	4.84	0.00390
93	8.1	5.57	4.88	0.00242
94	8.7	5.54	4.92	0.00321
95	7.3	5.72	4.97	0.00117
97	6.8	10.67	12.98	0.00013
98	15.2	11.39	13.06	0.01323
99	18.5	11.58	13.03	0.03193
100	14.2	14.52	12.75	0.02423
101	13.7	14.60	14.07	0.02042
102	14.1	15.13	14.11	0.02868
103	12.8	13.28	14.00	0.01740
104	16.8	17.04	14.82	0.04125
105	17.4	15.80	14.84	0.04606
106	18.2	15.62	14.74	0.06001
107	16.1	15.63	14.98	0.03783

Footnotes: 1) Total (Stage A + Stage B) whitecap coverage, as simple fraction; 2) Missing observations are those for which whitecap observations not recorded.